Frontier Energy System and Power Engineering
ISSN: 2720-9598

A Control Method for Modified Bidirectional Cuk DC-DC Converter

Muhammad Rifqi Azmi, Andriazis Dahono, Sofyan M. Ilman, Arwindra Rizqiawan, Pekik A. Dahono

School of Electrical Engineering and Informatics, Bandung Institute of Technology, Ganesha 10, Bandung, 40132, Indonesia
Corresponding: mrifqiazmi@students.itb.ac.id

Abstract

A control method for a modified bidirectional Cuk DC-DC converter is proposed in this paper. The proposed controller is a double control loop consisting of an inner current and a voltage control loop is used to control the converter. The small-signals model that is useful in designing controllers is derived in this paper. A simple PI controller is used for both controllers. The current controller is created separately from the voltage controller design to make the current response faster than the voltage response to make the controller work properly. The simulation and experimental results show that the proposed control method runs well to maintain stability with the battery application's bidirectional ability.

Keywords

DC-DC converter, Cuk Converter, Bidirectional, PI controller

INTRODUCTION

Indonesia is an archipelago country with more than 17,000 islands. Although Indonesia's electrification ratio is already reached more than 99% this year [1], many islands and remote areas still have no electricity access. Various programs have been run by the government to increase the electrification ratio in Indonesia. A microgrid is one of the possible solutions to overcome the problem.

A microgrid may be in the form of DC or AC. Figure 1 shows an example of a DC microgrid system used in this work. The energy sources may be coming from Photovoltaic (PV), small wind turbines, or small engines in practice. The DC microgrid is chosen here because of its simplicity compared to the AC microgrid since many renewable sources and Energy Storage System (ESS) generate DC voltages. Therefore, the number of converter stages can be reduced [2]. As can be seen in Figure 1, the DC microgrid uses a 400 V DC bus. A DC voltage of 400 V was selected because, with 400 V DC, converting to 220 V AC for standard household loads will be accessible using an inverter. PV modules, battery, and DC loads are connected to the DC bus using DC-DC converters. The DC-DC converter act as an interface between the battery and the bus. Therefore, the DC-DC converter must be capable of flowing power bidirectionally to allow charging and discharging.

Many methods were proposed using various bidirectional DC-DC power converters in [3]–[5]. In general, we can classify a bidirectional DC-DC power converter as isolated and non-isolated ones. The non-isolated DC-DC converter is preferred because of power loss consideration. In addition to high efficiency, the DC-DC converter has to produce a current with small ripple content to ensure the battery's long-term operation. Slobodan Cuk proposed a suitable converter for battery chargers and dischargers because it has continuous input and output currents with little ripple content, namely Cuk Converter [6]. Unfortunately, this converter has an output voltage with reversed polarity. This polarity can be a problem in practices.

A modified Cuk DC-DC converter was proposed a modified Cuk DC-DC converter in [7] [8] [9]. This converter has continuous input and output currents with unreversed polarity. It was shown that the modified Cuk DC-DC converter has bidirectional power capability with an efficiency that is higher than the conventional Cuk DC-DC converter. The efficiency is also higher than the traditional boost and buck-boost DC-DC converters. However, how to control the modified bidirectional Cuk DC-DC converter has not been discussed in the paper. To have a bidirectional capability, the controller needs to have a fast response to change the power direction quickly.

Frontier Energy System and Power Engineering
ISSN: 2720-9598

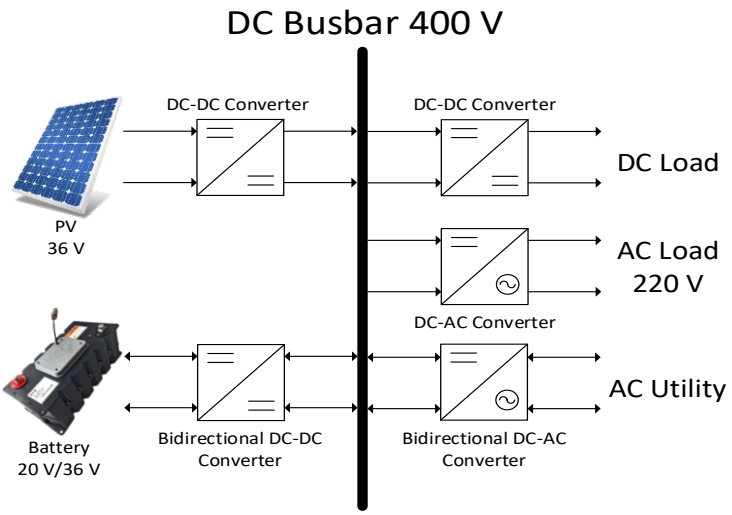

Fig. 1. DC microgrid system

This paper proposes a control scheme for the modified bidirectional Cuk DC-DC converter. A double loop controller consists of an inner loop current controller, and an outer loop voltage controller is used to control the converter. Small signal models that are useful in designing the controller are derived in this paper. Simple PI controllers are employed for both controllers. Simulated and experimental results are included in this paper to validate the performance of the proposed controller.

This paper explains a modified bidirectional Cuk DC-DC Converter in Section 2. Section 3 will discuss this converter's dynamic modeling to show the steps taken to design both the current and voltage controllers. Then, in Section 4, simulation and experimental results validate the proposed controller's performance is presented. Section 6 concludes the outcomes as well as the entirety of this paper.

BIDIRECTIONAL STEP-UP DC-DC MODIFIED CUK POWER CONVERTER

Figure 2 shows the conventional Cuk DC-DC converter proposed by Slobodan Cuk. This converter's main advantage is the continuous currents at the input and output sides caused by the inductors on both sides. A coupling capacitor is used to transfer energy. It is connected consecutively to the input and output side via the commutation of the transistor S_1 and S_2. The output voltage ratio in continuous conduction mode is

$$\frac{V_o}{E_d} = \frac{\alpha}{1-\alpha} \tag{1}$$

where $\alpha = \frac{T_{ON}}{T_S}$ is the duty cycle of transistor S, T_S is the switching period, V_o and E_d is the output and input voltage.

The disadvantages of the conventional Cuk DC-DC converter are the reversed output voltage polarity and has a voltage ratio that is not always greater than one, as we can see in Eq. (1). For the same duty cycle, the Cuk converter produces a lower voltage than the boost converter, which means the conventional Cuk DC-DC converter needs a higher duty cycle than a traditional boost converter. If a very high voltage ratio is desired, it will require an extreme duty cycle.

The suitable converter for DC microgrid application needs to have the following features: i) continuous input and output current, ii) unreversed voltage polarity, iii) high efficiency, and iv) moderate operating duty cycle. As is shown in [8], we can modify the conventional Cuk DC-DC converter into the one shown in Figure 3. Based on Figure 3, we can get a voltage ratio at the third terminal between E_d and V_o as follow

$$\frac{V_o}{E_d} = \frac{1}{1-\alpha} \tag{2}$$

This topology has the same voltage ratio as a conventional boost DC-DC converter. This topology requires a smaller duty cycle for the same output voltage as the conventional Cuk DC-DC converter. The efficiency is higher than the conventional Cuk, boost, and buck-boost DC-DC converters with unreversed polarity. Without eliminating the main advantage of conventional Cuk converters, it has a continuous current on both sides.

ISSN: 2720-9598

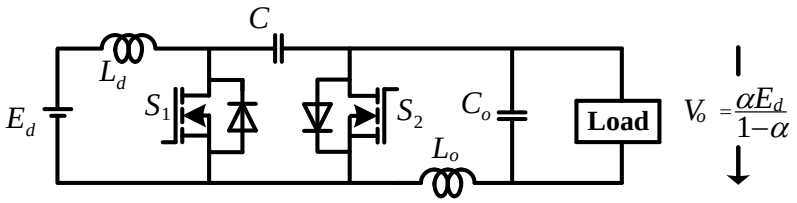

Fig. 2. Conventional Cuk DC-DC converter

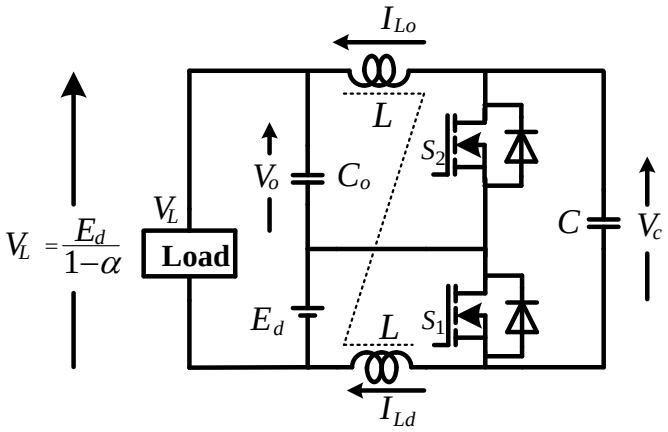

Fig. 3. Bidirectional modified Cuk DC-DC converter

DYNAMIC MODELING OF BIDIRECTIONAL MODIFIED CUK DC-DC CONVERTER

In applying a DC-DC converter as a switching mode power supply, it is desirable to provide a constant output voltage even when there are disturbances, such as input voltage and load variations. Therefore, we must equip the DC-DC converter with appropriate control methods. Various controllers for DC-DC converters have been proposed in the literature. Choudhary et al. developed a voltage controller for the Cuk DC-DC converter for photovoltaic power generation [10]. Chen proposed a combined controller (PI and sliding mode controls) to regulate a fourth-order Cuk converter in continuous conduction mode [11]. Chincholkar et al. designed an output feedback controller to handle the negative output Cuk converter [12]. We know that the most common control method is to control the duty cycle from the literature above. For its simplicity and robustness, the PI controller is chosen for this research. To be in bidirectional mode, the controller needs to control the direction of the power flow. To overcome the problem, the double-loop controller that controls the desired output voltage and the current flowing through the inductor is used.

This controller has an inner loop current controller and an outer loop voltage controller. To design the controller, the small-signal model of the converter is derived here. Figure 4 shows the double loop controller that is used in this paper. The load voltage is compared to the reference voltage to obtain the voltage error signal. The voltage error signal is processed by the voltage controller to determine the desired inductor current. The desired inductor current is then compared to the actual inductor current to resolve the inductor current error, which will then be processed by the current controller to determine the desired duty cycle. The desired duty cycle is then compared to a high-frequency carrier signal to determine the transistor's ON-OFF signals. Both voltage and current controllers are designed in such a way to make the current response much faster than the voltage response.

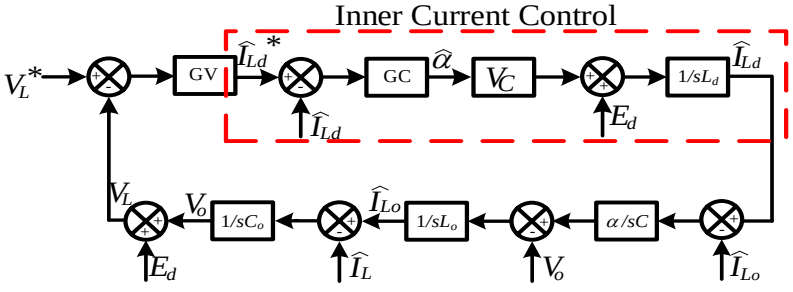

Fig. 4. Proposed Double Loop Controller

http://dx.doi.org/10.17977/um048v3i1p10-19

ISSN: 2720-9598

Current Loop Control Design

As the current controller is designed in such a way so that the response is much faster than the voltage response, we can create the current controller separately from the voltage controller design. There are two options for placing the current sensor, in the inductor on the input side (L_d) or the output side (L_o). Since the current control requires a fast response, the transfer function's order should be as small as possible. Assumed that the output of the coupling capacitor (V_C) is constant when the current in the inductor L_d is changed. Therefore, the dynamics of the voltage in the output capacitor and the current in the output inductor (C_o&L_o) are neglected. By using this assumption, the simplified system can be drawn, as shown in Figure 5. The transfer function will be in the first order as expected to have a fast performance.

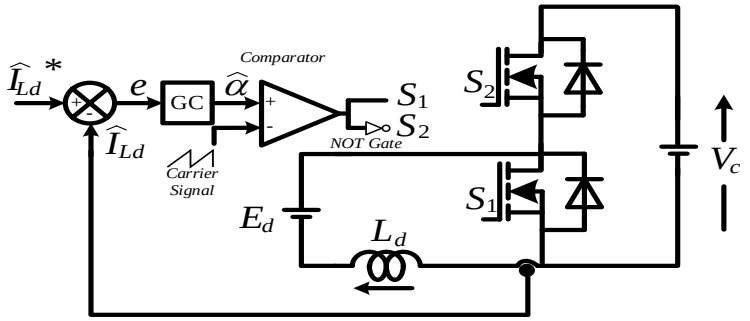

Fig. 5. The simplified system of the current control scheme

By using the simplified system in Figure 5, the small-signal model, and the transfer function of $\frac{\hat{I}_{Ld}}{\hat{\alpha}}$ as follow:

$$[sL_d]\,\hat{I}_{Ld} = [V_C]\,\hat{\alpha} + \hat{E}_d \tag{3}$$

$$\frac{\hat{I}_{Ld}}{\hat{\alpha}} = \frac{V_C}{(L_d)s} \tag{4}$$

The converter will be operated in critical conduction mode (CCM) to make the converter respond faster. It means that the inductor value is minimal, making it more responsive to any change in the reference signal. Table 1 summarizes all the design parameters for the converter used in this research.

TABLE I
CONVERTER DESIGN PARAMETER

Component	L_d	L_o	C	C_o	V_C	V_o	E_d	f
Value	$1.375e^{-4}$ H	$1.375e^{-4}$ H	10^{-4} F	10^{-4} F	40 V	40 V	20 V	10 kHz

Using the values in Table 1 into Eq. (4), we will get the L_d inductor current to the duty cycle transfer function Eq. (5).

$$\frac{\hat{I}_{Ld}}{\hat{\alpha}} = \frac{40}{(1.375e^{-4})s} \tag{5}$$

Figure 6 shows a small signal block diagram of the current loop control. The transfer function of the PI-controller is defined by Eq. (6), where K_P and K_i is the gain.

$$K_p + \frac{K_i}{s} = \frac{K_p\,(s+\frac{K_i}{K_p})}{s} \tag{6}$$

Therefore, the transfer function $\frac{\hat{I}_{Ld}}{\hat{I}_{Ld\_ref}}$ will be,

$$\frac{\hat{I}_{Ld}}{\hat{I}_{Ld\_ref}} = \frac{(Kp)\,(40)\left(s+\frac{Ki}{Kp}\right)}{s\left(1.375e^{-4}s\right)} \tag{7}$$

In the equation, Eq. (7) is a transfer function of the small actual current signal from L_d inductor to the reference current using a PI controller. The results obtained are valid for a specific operating point.

ISSN: 2720-9598

By using a commonly used procedure to determine K_p and K_i, we can determine the current control parameter values. The response of the current controller must be much faster than the response of the voltage controller. By substituting the final equations from gain and phase margin condition, it is obtained $K_p = 5.8, K_i = 50889.56$, and $T_i = 1.139e^{-4}$. Figure 7 shows the bode plot diagram of the current controller. It is shown that the current controller has a bandwidth of approximately 100 kHz.

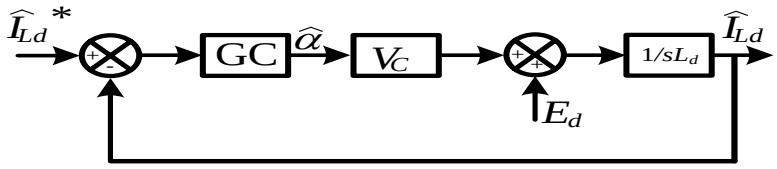

Fig. 6. Current control loop diagram

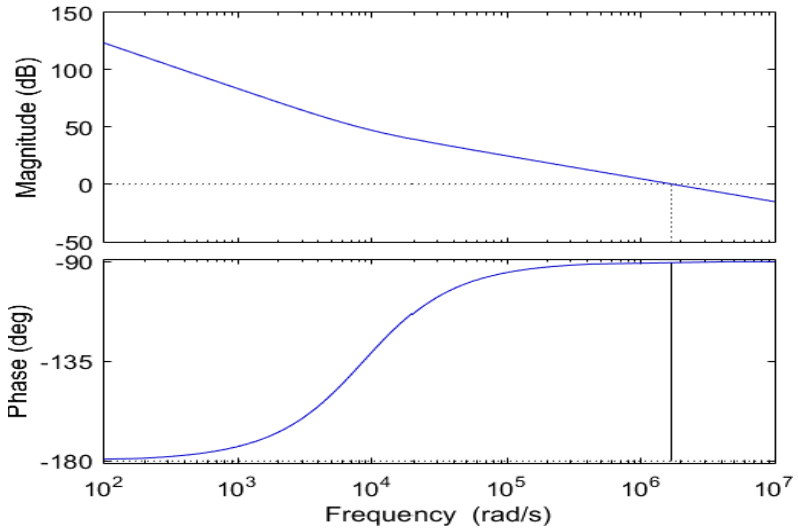

Fig. 7. Bode plot diagram of actual current against a reference current

Voltage Loop Control Design

Since the voltage controller does not require a fast response because the load variation is usually slow, then the output currents are assumed to be fixed. The current inductor on the input side (I_{Ld}) is already steady (refers to the current control analysis in the previous session). Therefore, we can be neglect I_{Ld} loop dynamics and the transfer function will be in third-order. Figure 8 shows the simplified system for voltage loop design. A controlled current source replaces the I_{Ld} loop dynamics. The current source replaces the load loop dynamics with the consistent voltage polarity direction with the original circuit. Figure 9 shows the voltage loop block diagram omitting the inner current loop. Eq. 8 shows the small-signal matrix of this control design.

$$\begin{bmatrix} sL_o & -\alpha & 1 \\ \alpha & sC & 0 \\ -1 & 0 & -sC_o \end{bmatrix} \begin{bmatrix} \hat{I}_{Lo} \\ \hat{V}_C \\ \hat{V}_o \end{bmatrix} = \begin{bmatrix} 0 \\ \alpha \\ 0 \end{bmatrix} \hat{I}_{Ld} + \begin{bmatrix} V_c \\ I_{Lo} \\ 0 \end{bmatrix} \hat{\alpha} \tag{8}$$

$$\frac{\hat{V}_o}{\hat{I}_{Ld}} = \frac{\alpha^2}{(L_o)(C)(C_o)s^3 + (C + (\alpha^2)(C_o))s} \tag{9}$$

The transfer function of $\frac{\hat{V}_o}{\hat{I}_{Ld}}$ Can be seen in Eq. (9). After entering the values in Table 1 into Eq. (9), we will get the $\frac{\hat{V}_o}{\hat{I}_{Ld}}$ Transfer function in Eq. (10). The closed-loop $\frac{\hat{V}_o}{\hat{V}_{o\_ref}}$ PI-controller is shown in Eq. (11).

$$\frac{\hat{V}_o}{\hat{I}_{Ld}} = \frac{0.25}{1.375e^{-12}s^3 - 1.25e^{-4}s} \tag{10}$$

$$\frac{\hat{V}_o}{\hat{V}_{o\_ref}} = \frac{(Kp)\,(0.25)\left(s + \frac{Ki}{Kp}\right)}{s\,(1.375e^{-12}s^3 - 1.25e^{-4}s)} \tag{11}$$

By using a commonly used procedure to determine K_p and K_i, we can determine the voltage parameter values. By substituting the final equations from gain and phase margin condition, it is obtained $K_p = 4.89, K_i = 2055.31$, and $T_i = 2.37e^{-3}$. Figure 10 shows the bode plot diagram of the current controller. It

http://dx.doi.org/10.17977/um048v3i1p10-19

ISSN: 2720-9598

is shown that the current controller has a bandwidth of approximately 3 kHz. This bandwidth is much smaller than the current control bandwidth. Thus, the voltage controller's response is slower than the current controller's response so that the controller will work properly.

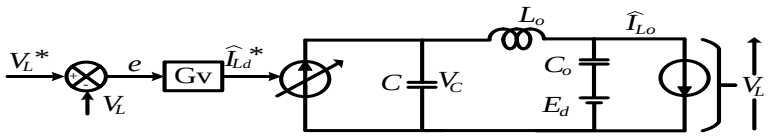

Fig. 8. The simplified system of the voltage control scheme

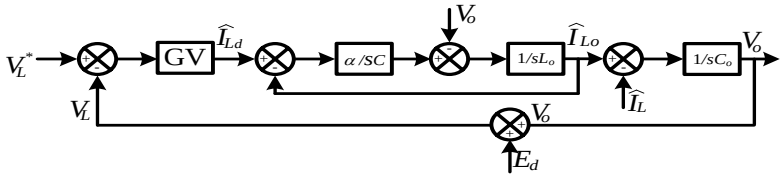

Fig. 9 Voltage loop control diagram

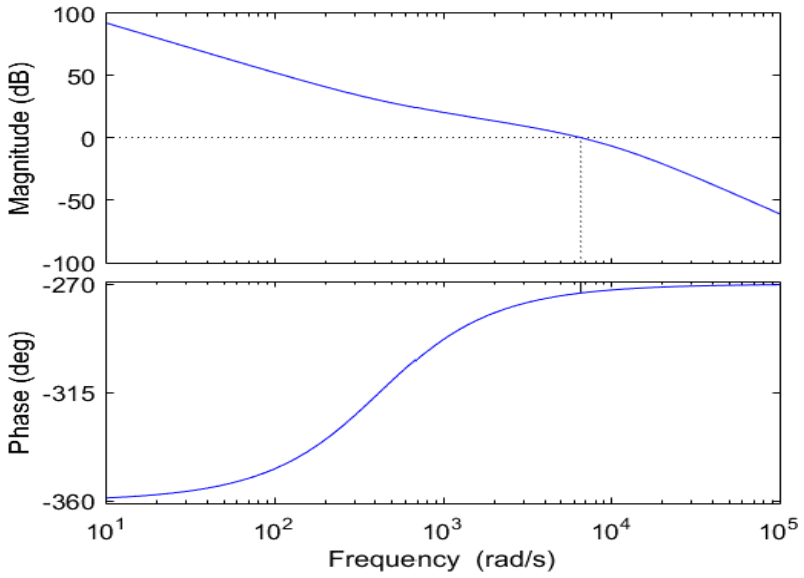

Fig. 10. Bode plot diagram of actual voltage against a reference voltage

SIMULATED AND EXPERIMENTAL RESULTS

This section will discuss the simulation and experiment results to validate the performance of the proposed controller. The component values used are the same as in Table 1. Figure 11 shows the simulation scheme of double-loop control.

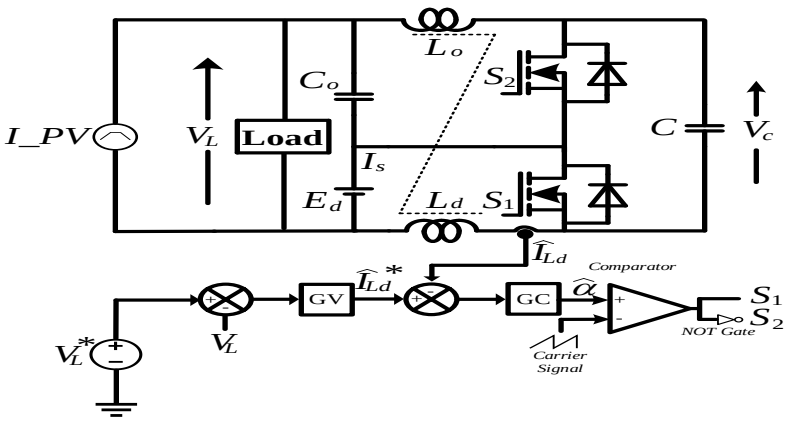

Fig. 11. Converter Simulation Circuit (Closed Loop)

http://dx.doi.org/10.17977/um048v3i1p10-19

ISSN: 2720-9598

Simulated Results

The modified bidirectional Cuk DC-DC converter was simulated using PSIM with a double-loop PI controller. The converter was simulated for three different cases to see the effectiveness of the controller employed. These three scenarios are the following. The variations in input supply voltage and load resistance were simulated using step changes.

1) Variation in input supply voltage.
2) Variation in load resistance.
3) Bidirectional mode.

- **Variation in input supply voltage**

In this case, the effect of input supply voltage variation (step change) is analyzed. The variation in input supply voltage (battery) possibly happens when the load is suddenly increasing. When the load is rising, the current demand is also rising, making the battery voltage drop.

Figure 12 shows the simulation results of the output voltage (V_o), input voltage (E_d) when the input voltage changes (from 20 V to 17 V) at $t = 0.3s$ and returns to normal at $t = 0.31s$. It can be seen that the controller can maintain the desired output voltage when the input voltage changes with the actual current in the inductor L_d, which rapidly follows the change in the reference current. When the input voltage changes, the output voltage drops. With a fast controller response, the voltage drop is not too long and quickly returns to the desired voltage.

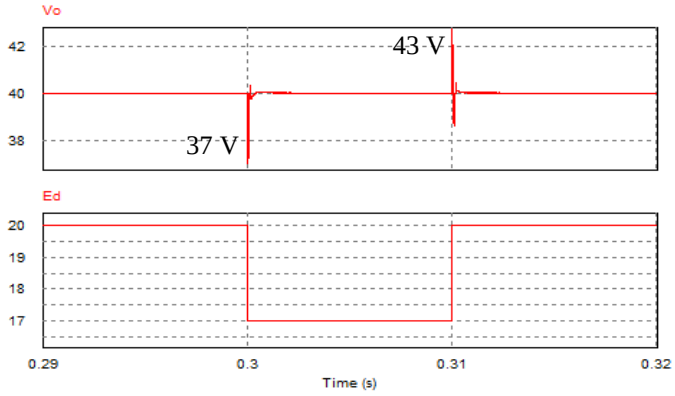

Fig. 12. The load voltage ($\boldsymbol{V_o}$), source voltage ($\boldsymbol{E_d}$) when the source voltage changes

- **Variation in load resistance**

In this case, the effect of load resistance variation is analyzed. This simulation aims to prove that the load can be added or diminished as needs without changing the output voltage. In this simulation, the load changes from 22 Ω to 9 Ω.

Figure 13 shows the output voltage waveform when the load resistance is changing. The load resistance decreases during the time $t = 0.3s$. This variation has a noticeable effect on the output voltage. The output voltage of the converters drops at $t = 0.3s$. As we can see, when there is a load change, the output current is increased and following by the output voltage drop, which only lasts for $0.01s$, which is still acceptable in control theory.

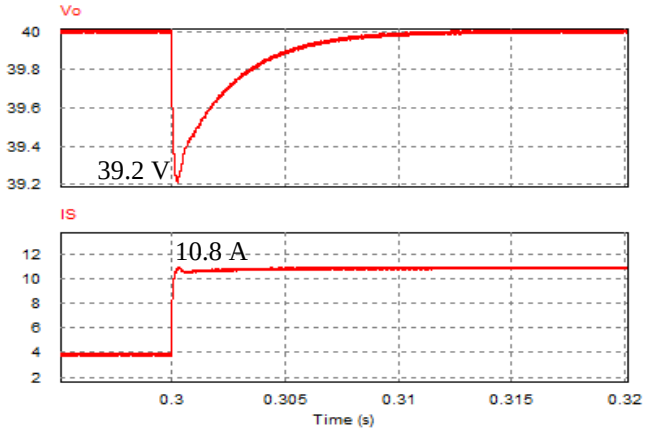

Fig. 13. Output voltage when the load changes

http://dx.doi.org/10.17977/um048v3i1p10-19

ISSN: 2720-9598

- **Bidirectional mode (battery charge and discharge)**

In this simulation, the authors will use the bidirectional modified Cuk DC-DC converter as a battery charger and discharger in the DC microgrid system. The battery voltage (E_d) used in this system is the 20 V to represent a low State of Charge (SoC) battery condition. To achieve the DC bus voltage at 400 V, ten converters, each has an output voltage of 40 V, are connected in series.

In the DC microgrid, the converter on the battery act as the DC bus voltage keeper. The converter on the PV acts as a current source due to the Maximum power point tracker (MPPT) application typically employed in PV's converter. If the DC microgrid is on-grid (connected to the utility), the utility act as the DC bus voltage keeper through a rectifier. The converter on the battery responsible for smoothing the power fluctuation due to the PV. If the battery is full, the PV's converter can not run because the bus can no longer receive power. If the bus can still receiving power, then the battery voltage is not full.

Figure 11 shows the bidirectional simulation scheme for battery application. Charging occurs when the PV produces excess power so that the battery can absorb it. When there is no sufficient supply from PV (little sunshine/cloudy weather), the battery is responsible for supplying electricity to the load to replace the PV. In this simulation, PV is modeled as a fluctuating current source (MPPT) that connects parallelly with the load. It aims to prove that the converter is designed to work in bidirectional mode. We can see the simulation result in Figure 14. It shows the simulation results when the current generated by PV is varying. The PV is modeled as a trapezoidal wave (I_{PV}). When the PV's current (trapezoidal wave is increased and decreased slowly), the controller will maintain the load voltage by taking excess energy to charge the battery (negative current source). When there is no PV current (trapezoidal wave is 0), the energy shortage is met by taking battery energy to meet the load requirements (positive current source).

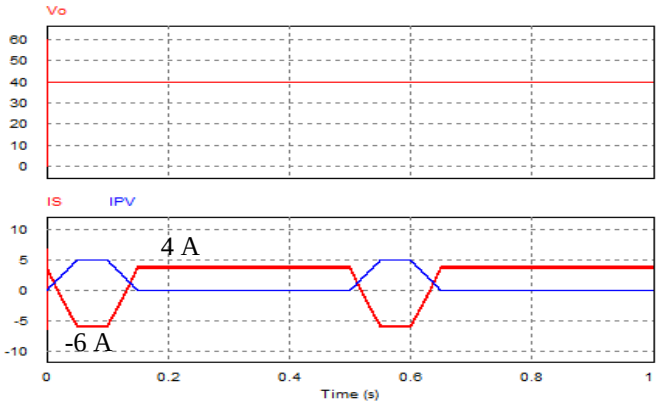

Fig. 14. Output voltage ($\boldsymbol{V_o}$) and source currents ($\boldsymbol{I_S}$) when the PV current changes

Experimental Results

Experiments are an essential thing to do to validate the performance of this converter. The DC source is obtained from a DC power supply that is maintained at 36 V.

- **Current control experiment**

Figure 15 shows the output, inductor (L_d), and reference current. The purpose of this experiment is to observe the current control in the inductor (L_d). The test was carried out when the converter output current varied. When the load changes, the converter output, and the inductor current (L_d) will also change. By using current control, the inductor current will follow the reference current.

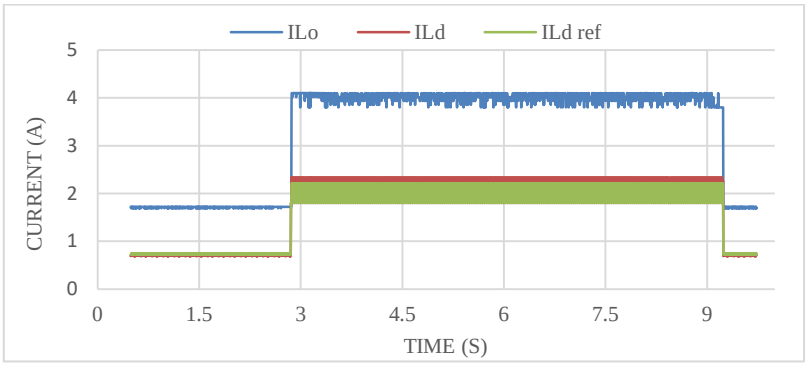

Fig. 15. The experiment result of current control (I_{Ld}) when the load changes

http://dx.doi.org/10.17977/um048v3i1p10-19

ISSN: 2720-9598

- **The load is changed**

Figure 16 shows the output voltage, input voltage, reference, and output current during a load change. When the load is changing, it will drop the output voltage, and automatically, the output current will rise to keep the power at the same value. As we can see, the output voltage can still follow the setpoint with the changing load, although there is a slight voltage drop.

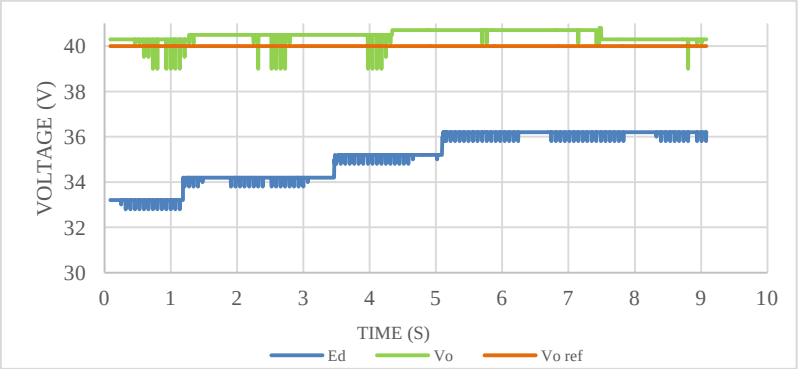

Fig. 16. The experiment result of output voltage with fluctuating input voltage

- **The input voltage is changed**

Figure 17 shows the output voltage, reference, and fluctuate voltage input (33 V – 36 V). The output voltage can still follow the setpoint with the fluctuating voltage input. In other words, the controller is running well.

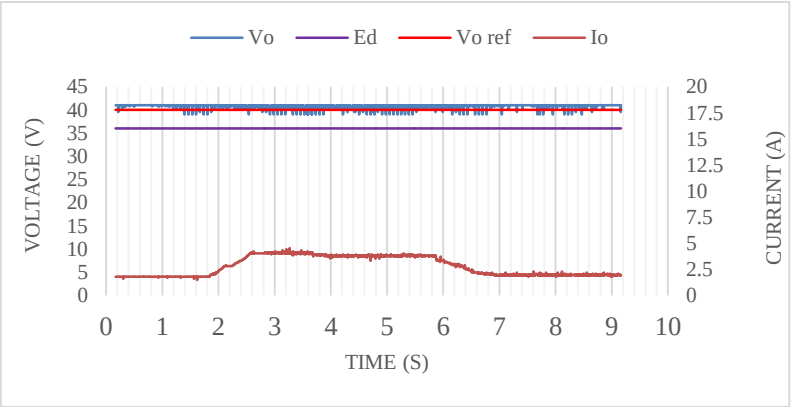

Fig. 17. The experiment result of output voltage during load changes

- **Bidirectional mode**

Figure 18 shows the current through the inductor L_d when the power flow is reversed. In this experiment, we connected another DC voltage source connected in parallel to the load. To make the power flow is changed, the duty cycle of the power converter is then adjusted. This figure shows the bidirectional power flow capability of the proposed power converter.

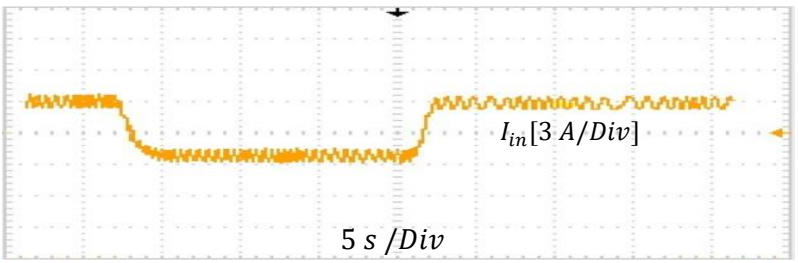

Fig. 18. Inductor L_d current when the power flow is positive and negative

CONCLUSION

A control method for a modified bidirectional Cuk DC-DC converter is proposed in this paper. This topology has the same voltage ratio as a conventional boost DC-DC converter. This topology requires a smaller duty cycle for the same output voltage as the conventional Cuk DC-DC converter. The efficiency is

higher than the conventional Cuk, boost, and buck-boost DC-DC converters with unreversed polarity. Without eliminating the main advantage of conventional Cuk converters, it has a continuous current on both sides. It may connect the DC bus's energy storage device as an interface converter, working in positive and negative current modes to transfer the bidirectional energy flow. The simulation and experimental results show that the proposed control method runs well to maintain stability with the battery application's bidirectional ability.

ACKNOWLEDGMENTS

The authors wish to thank the Ministry of Research, Technology, and Higher Education of Indonesia, LPDP, PT.LEN Industry and KOMIPO for providing research funds for this work. The author would like to acknowledge the contribution of Mrs. Tri Ardriani in assisting in editing this paper

REFERENCES

[1] PT PLN;, "Memaknai Tantangan, Meningkatkan Layanan Redefining Challenges, Enhancing Services," *Laporan Tahunan*, pp. 175–176, 2019, [Online]. Available: https://web.pln.co.id/statics/uploads/2020/07/PLN_AR_2019_OJK_Med_260620.pdf.

[2] D. Kumar, F. Zare, and A. Ghosh, "DC Microgrid Technology: System Architectures, AC Grid Interfaces, Grounding Schemes, Power Quality, Communication Networks, Applications, and Standardizations Aspects," *IEEE Access*, vol. 5, no. August, pp. 12230–12256, 2017, doi: 10.1109/ACCESS.2017.2705914.

[3] K. Bhatt, R. A. Gupta, and N. Gupta, "Comparative Analysis and Control of Bidirectional DC-DC Converters," *2019 IEEE 1st International Conference on Energy, Systems and Information Processing, ICESIP 2019*, no. 1, 2019, doi: 10.1109/ICESIP46348.2019.8938349.

[4] W. C. Liao *et al.*, "Study and implementation of a novel bidirectional DC-DC converter with high conversion ratio," *IEEE Energy Conversion Congress and Exposition: Energy Conversion Innovation for a Clean Energy Future, ECCE 2011, Proceedings*, pp. 134–140, 2011, doi: 10.1109/ECCE.2011.6063760.

[5] G. Stahl, M. Rodriguez, and D. Maksimovic, "A high-efficiency bidirectional buck-boost DC-DC converter," *Conference Proceedings - IEEE Applied Power Electronics Conference and Exposition - APEC*, pp. 1362–1367, 2012, doi: 10.1109/APEC.2012.6165997.

[6] S. Cuk, "A New Zero-Ripple Switching DC-to-DC Converter and Integrated Magnetics," *IEEE Transactions on Magnetics*, vol. 19, no. 2, pp. 57–75, 1983, doi: 10.1109/TMAG.1983.1062238.

[7] A. Dahono, A. Rizqiawan, and P. A. Dahono, "A modified Cuk DC-DC converter for DC microgrid systems," vol. 18, no. 6, 2020, doi: 10.12928/TELKOMNIKA.v18i6.16466.

[8] S. M. Ilman, A. Dahono, M. A. K. Prihambodo, B. A. Y. Putra, A. Rizqiawan, and P. A. Dahono, "Analysis and Control of Modified DC-DC Cuk Converter," *Proceedings of the 2nd International Conference on High Voltage Engineering and Power Systems: Towards Sustainable and Reliable Power Delivery, ICHVEPS 2019*, pp. 1–6, 2019, doi: 10.1109/ICHVEPS47643.2019.9011054.

[9] Dahono, Andriazis and P. A. Dahono, "A Comparative Evaluation of Bidirectional Step-Up DC-DC Converters," *International Journal on Electrical Engineering and Informatics*, vol. 12, no. 2, pp. 338–397, 2020, doi: 10.15676/ijeei.2020.12.2.1.

[10] P. Choudhary and S. N. Mahendra, "Feedback control and simulation of DC-DC Cuk converter for solar photovoltaic array," *2016 IEEE Uttar Pradesh Section International Conference on Electrical, Computer and Electronics Engineering, UPCON 2016*, pp. 591–596, 2017, doi: 10.1109/UPCON.2016.7894721.

[11] Z. Chen, "PI and sliding mode control of a Cuk converter," *IEEE Transactions on Power Electronics*, vol. 27, no. 8, pp. 3695–3703, 2012, doi: 10.1109/TPEL.2012.2183891.

[12] S. Chincholkar and C. Y. Chan, "Design and implementation of an output feedback controller for the Cuk converter," in *IECON 2015 - 41st Annual Conference of the IEEE Industrial Electronics Society*, 2015, pp. 86–90, doi: 10.1109/IECON.2015.7392080.